EUROPEAN ORGANIZATION FOR NUCLEAR RESEARCH

DI/HP/165
Health Physics Group
25 May, 1973

DOSIMETRY PROBLEMS OF NEGATIVE π MESONS

J. Baarli and A.H. Sullivan

CERN, Geneva
Switzerland

1. INTRODUCTION

Negative pions are of interest for radiotherapy on account of their promising depth-dose distribution and the possible high RBE of the charged secondaries produced in the nuclear interactions occurring at the end of their range.

The intensities of existing pion beams have so far excluded their application to radiation therapy but have permitted limited radiobiological studies and allowed some investigation into dose measurement methods.

CERN has a modest programme of radiobiological investigations which include the effect of negative pions on mice (spermatogonia survival) and Vicia Faba roots (10 days growth). The dosimetry necessary for these investigations has shown the problems that exist in trying to estimate absorbed dose to the biological specimens in the radiation field of a stopped negative pion beam.

Invited paper to be presented at
XIIIth International Congress of Radiology
Madrid, 15-20 October, 1973

2. PROPERTIES OF PION BEAMS

The properties of pions and the kinetics of their interactions have been extensively reviewed and many computations made in an attempt to assess the influence of various parameters on the applicability of pions to radiation therapy[1-5]. Computations of the charged particle types and spectra produced in pion interactions have been made using an intranuclear cascade model[6], which gives an indication of the secondaries that may be produced; these are listed in Table 1 for carbon. As can be seen from this table, over 80% of the energy of charged secondaries is expected to be carried off by protons and alpha particles with mean energies of about 20 and 15 MeV.

The results of absorbed dose measurements when a beam of negative pions is stopped in tissue-equivalent plastic is shown in Fig. 1.

The main peak in this depth-dose curve is due to pion interactions together with the Bragg peak of the slowing down charged pions. The smaller peak after the main peak is due to stopping muons (of the same initial momentum as the pions). Electron contamination of the beam can be seen as the dose beyond the stopped muon peak. The form of this curve depends on the beam optics used, the momentum spread of the pions and the amount of contamination. The depth-dose curve is also a function of the absorber used. The influence of momentum spread and beam diameter on the shape of the depth-dose curve has been investigated theoretically[7]. These calculations show that the smaller the momentum spread, the narrower the stopped pion peak and the greater the contribution of the pion interaction secondaries to the peak dose.

Experience shows that the parameters that best describe the depth-dose curves are:

- beam half-width,
- peak depth,
- ratio peak/entrance dose,
- peak width at 80% height.

The proportion of dose from nuclear interactions can be inferred from Fig. 2, which shows the depth-dose distributions from negative and positive pions of the same momentum. In the latter the peak dose is due to pion slowing down with a small contribution from pion decay (approximately 7 MeV locally from the decay muon and electron). It is also interesting to note that the largest difference between these two curves and hence the nuclear interaction dose occurs at the back edge of the negative pion peak.

Measurements in the stopped pion region indicate that at the peak dose, 45% of the energy deposited in tissue-equivalent plastic originates from pion interactions, 40% is due to pion ionization, and the rest is contamination[8].

3. PROBLEMS OF DOSIMETRY

Computations and measurements indicate that the spectra of secondary charged particles produced in pion interactions depend on the nucleus with which the interaction takes place. Hence a dosimeter must be of a material where the nuclear interaction products as well as the stopping power for charged particles is known, in order that the necessary corrections can be made to determine the dose in tissue from the dosimeter reading.

The most direct method of dosimetry would be to use a tissue-equivalent ionization chamber. Several factors have to be taken into account in the design of an ionization chamber for measurement of the dose from stopped negative pions.

Tissue-equivalent plastics used for ionization chambers contain an excess of carbon in place of oxygen in tissue. This difference in composition or "non tissue equivalence" will affect the response of the dosemeter to stopped negative pions. The probability of pion capture by a nucleus is proportional to its charge[9]. A capture by hydrogen is quickly transferred to a larger nucleus. Using the computed data of Guthrie et al.[6] and the

experimental data obtained using emulsions by Fowler and Mayes[9] for the secondary particle energies per capture in various elements, it is possible to estimate the corrections necessary. The estimated energy deposition per stopped pion in dosimetric materials and tissue is given in Table 2. Although the computed secondary particle spectra give an overall picture of a pion interaction it is doubtful whether they are sufficiently accurate to assess small differences in the energy liberated between different capturing elements when these differences are only a small fraction of the 140 MeV involved in the interaction. Both the computed and measured energy deposition indicate that a correction is necessary which is estimated to be of the order of 5-10%.

Typical dose-rate variations with depth and isodose contours found with a symmetrically focussed beam are shown in Fig. 3. The position of a 1 cm radius sphere (which is the order of volume over which a reasonably uniform dose can be determined in a stopped pion peak) is also indicated in the figure. If this solid is replaced by a gas volume, as may be the case when ionization chambers are used, then the radiation field will be perturbed. The proportion of charged particle energy that is deposited within a given distance from the site of an interaction in water is shown in Fig. 4 [10]. As can be seen, 50% of the energy deposited is at distances greater than 0.7 mm (700 microns) from the site of pion capture. As the stopped pion region is relatively small and the secondaries are isotropically emitted, energy will be transported through the gas away from the position of maximum interaction rate. Hence, unless the gas volume is small compared to the dimensions of the peak, the dose measured will not necessarily be the same as the average in the solid that the gas volume has replaced. The magnitude of the correction necessary with a parallel-plate ionization chamber depends on the ratio of beam diameter to electrode spacing and diameter of the collector electrode, as well as to some extent on gas pressure. It is calculated that the problem is largely avoided if the width of the pion beam is greater than 10 times the plate spacing.

Another consideration with ionization chambers is the variations that occur in energy loss per ion pair produced in the gas for the different charged particles emitted from pion interactions. Estimated corrections to the w value for the different secondaries are given in Table 1. These are estimated on the basis of an ionization defect model. The mean value is only about 2% higher than that for electrons. This correction is small as the majority of energy is deposited by protons and alpha particles of relatively high initial energy.

4. DISCUSSION

A series of measurements of depth-dose curves with pion beams in water or tissue-equivalent plastic have been made at CERN for radiobiology experiments[8,11]. A typical beam had the following parameters:

- pion energy = 90 MeV
- peak dose-rate = 2.8 rad/h
- beam half-width = 5 cm
- peak depth = 22.2 g/cm^2
- width of stopped peak (at 80% max. dose) = 2.5 g/cm^2
- % dose from contamination in peak = 13%

The dosimeter used was a parallel-plate tissue-equivalent chamber which is shown diagrammatically in Fig. 5. The collector diameter (2 cm) is chosen to correspond to the usable cross-section of the pion peak as illustrated in Fig. 3. The plate spacing is 2.3 cm, making the sensitive volume about 9 cm^3. This volume is necessary on account of the requirement to measure the low dose-rates in the CERN pion beams.

The design of the dosimeter used is not ideal and a much smaller sensitive volume would be desirable. A dosimeter of parallel-plate design seems the best configuration as the depth of the sensitive volume in the stopping material is then well

defined. A chamber with variable plate spacing so that extrapolation to zero gas volume can be made would be ideal. The electrodes should be of tissue-equivalent plastic and at least 1 cm thick to ensure that the whole pion stopping region is in the material of the chamber. The corrections necessary with such a chamber to take account of the composition of the chamber and uncertainties in the ω values would then be less than 10%. Use of other dosimeters, such as solid-state detectors or plastic scintillators, would require considerable detailed investigation into their response relative to tissue.

Radiobiological measurements indicate that the maximum "effect rate" in a stopped pion peak may not coincide with the peak absorbed dose, which is consistent with the fact that the nuclear interaction concentration is higher on the back edge of the stopped pion peak[12]. Hence it may be questionable whether absorbed dose alone is sufficient for optimizing therapeutic exposure conditions. Another parameter which would be of interest is the spatial distribution and location of the maximum pion stopping rate. This parameter together with absorbed dose-rate may be necessary in order to adjust the position of any tumour for a treatment using a stopped negative pion beam.

REFERENCES

1. P.H. Fowler and D.H. Perkins, Nature 189, 524 (1961).

2. M.R. Raju and C. Richman, Current Topics in Radiation Research 8, 159 (1972).

3. S. Curtis and M.R. Raju, Rad. Res. 34, 239 (1968).

4. T.W. Armstrong and K.C. Chandler, Rad.Res. 52, 247 (1972).

5. J. Turner et al., Rad. Res. 52, p. 229 (1972).

6. M.P Guthrie, R.G. Alsmiller and H.W. Bertini, Nucl. Instr. and Methods 66, 29 (1968).

7. J. Turner et al., Proc. Int. Congr. on Protection against Accelerator and Space Radiation, CERN 71-16, Vol. 1, p. 231 (1971).

8. A.H. Sullivan and J. Baarli, Phys.Med.Biol. 13, 435 (1968).

9. P.H. Fowler and V.M. Mayes, Proc.Phys.Soc. 92, 377 (1967).

10. J. Dutrannois, R.N. Hamm, J.E. Turner and H.A. Wright, Phys. Med. Biol. 17, 765 (1972).

11. J. Baarli, A.H. Sullivan, M. Bianchi and M. Quintiliani, Proc. Int. Congr. on Protection against Accelerator and Space Radiation, CERN 71-16, p. 133 (1971).

12. J. Baarli and M. Bianchi, Int. J. Radiat. Biol. 22, 183 (1972).

FIGURE CAPTIONS

Fig. 1. Depth-dose curve for negative pions in tissue-equivalent plastic.

Fig. 2. Comparison of negative and positive pion depth-dose distributions indicating the location of dose from nuclear interactions.

Fig. 3. Variation of dose with depth and dose contours at the peak dose in tissue-equivalent plastic.

Fig. 4. Per cent of energy deposited within a given distance from the site of a pion interaction.

Fig. 5. Cross-section of the parallel-plate tissue-equivalent ionization chamber used for pion dosimetry.

Table 1

Charged products from pion capture (in carbon)

Particle	Energy per interaction		Average energy of particle	Energy per ion pair ω/ω_o
	MeV	% of total	MeV	
Proton	20	47	20	1.00
Deutron	2.8	6.6	11	1.02
Triton	1.0	2.3	13	1.02
^{3}He	0.3	0.7	13	1.02
Alpha	17	40	15	1.03
Li	1.22	2.9	6	1.1
Be	0.16	0.38	3	1.3
B	0.13	0.3	2	1.5

Table 2

Energy deposition in dosimetric materials based on computed and measured energy distribution of charged particles

Material	Local energy deposition per stopped pion	
	Calculated	Measured
	MeV	MeV
Tissue	37.3	27.3
T.E.Plastic	41.9	28.5
T.E.Gas	40.0	28.3

FIG.1

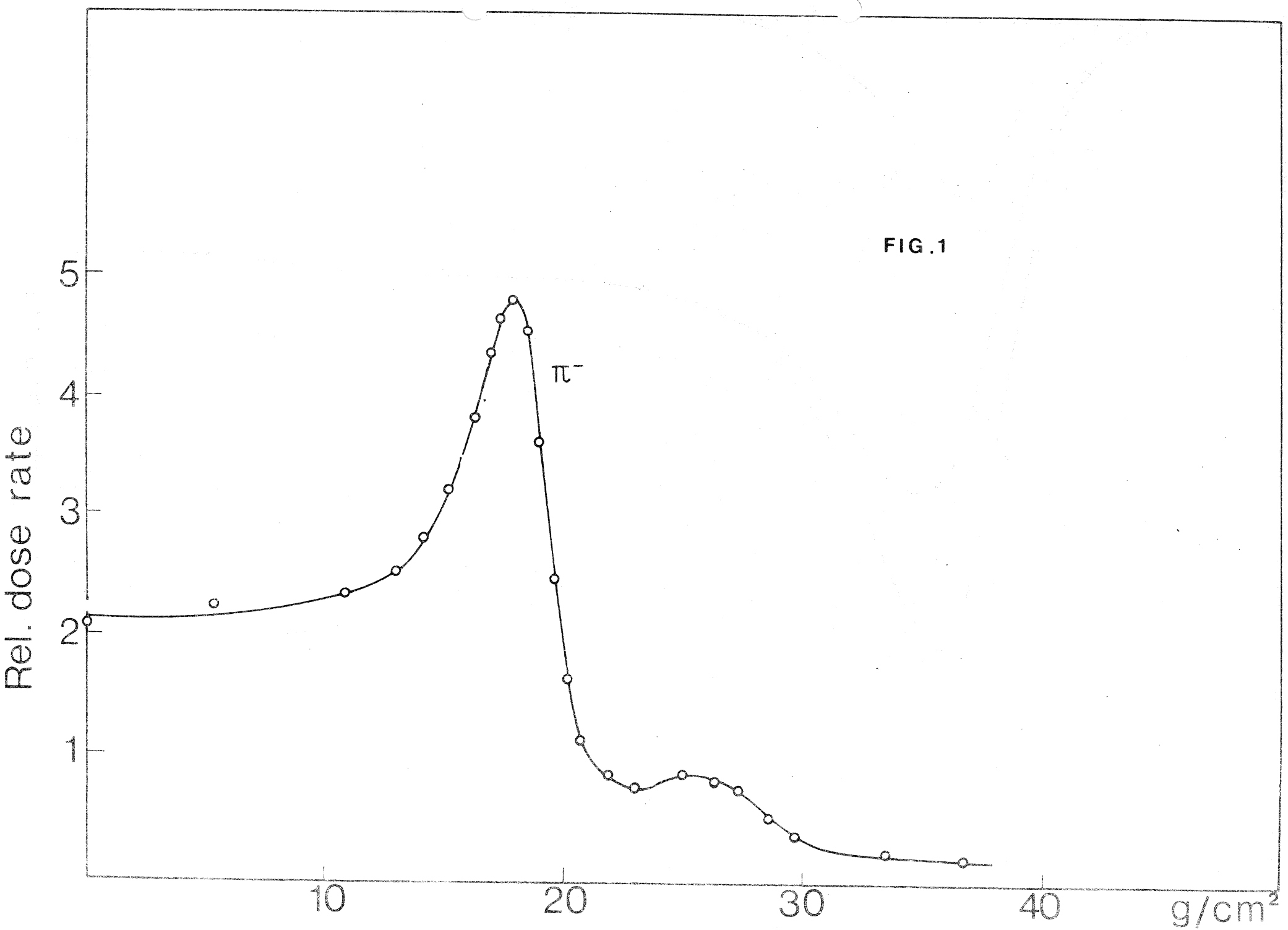

FIG. 2

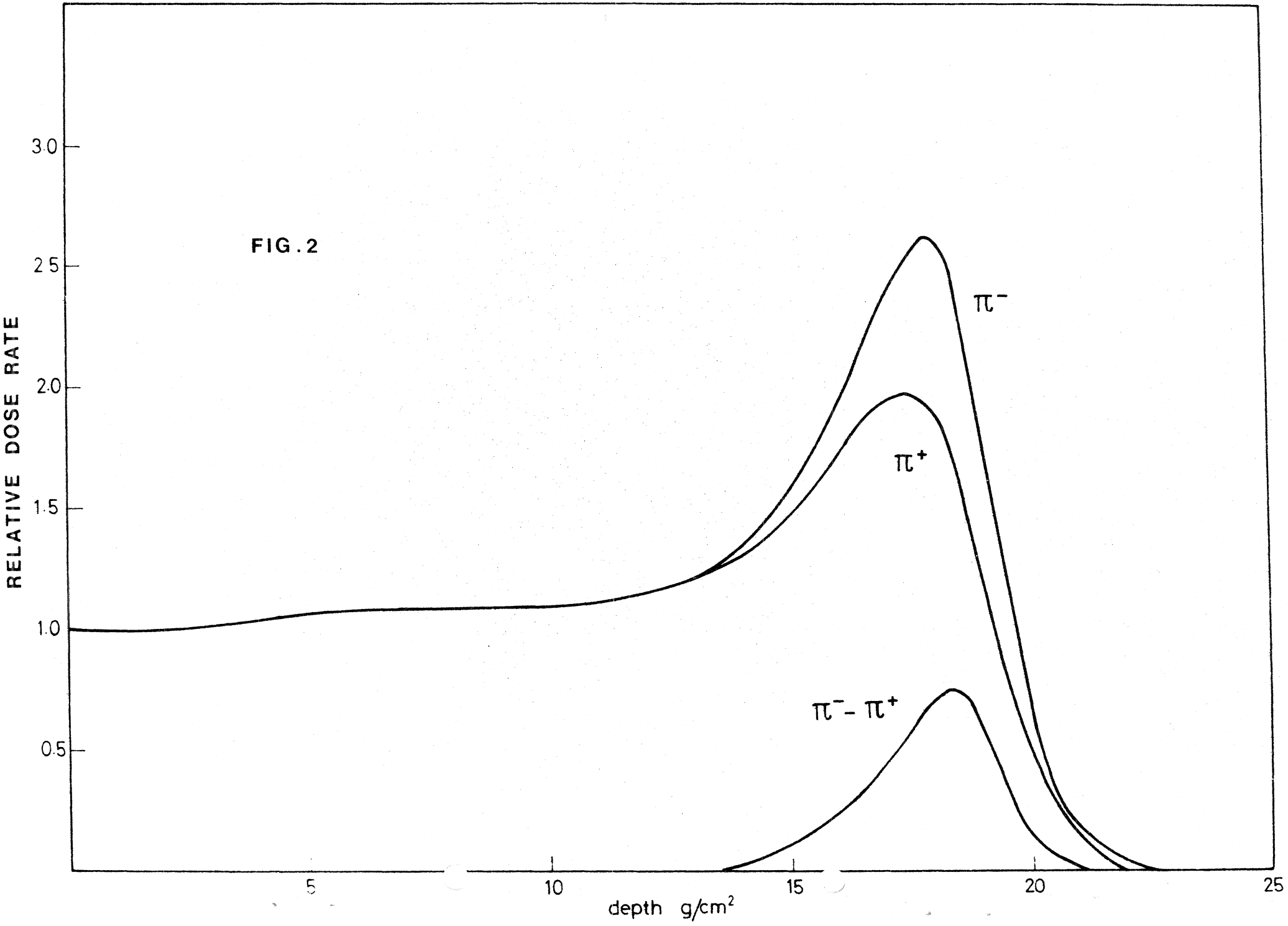
RELATIVE DOSE RATE
3.0
2.5
2.0
1.5
1.0
0.5
π⁻
π⁺
π⁻ - π⁺
5
10
15
20
25
depth g/cm²

a) dose rate variation with depth near peak

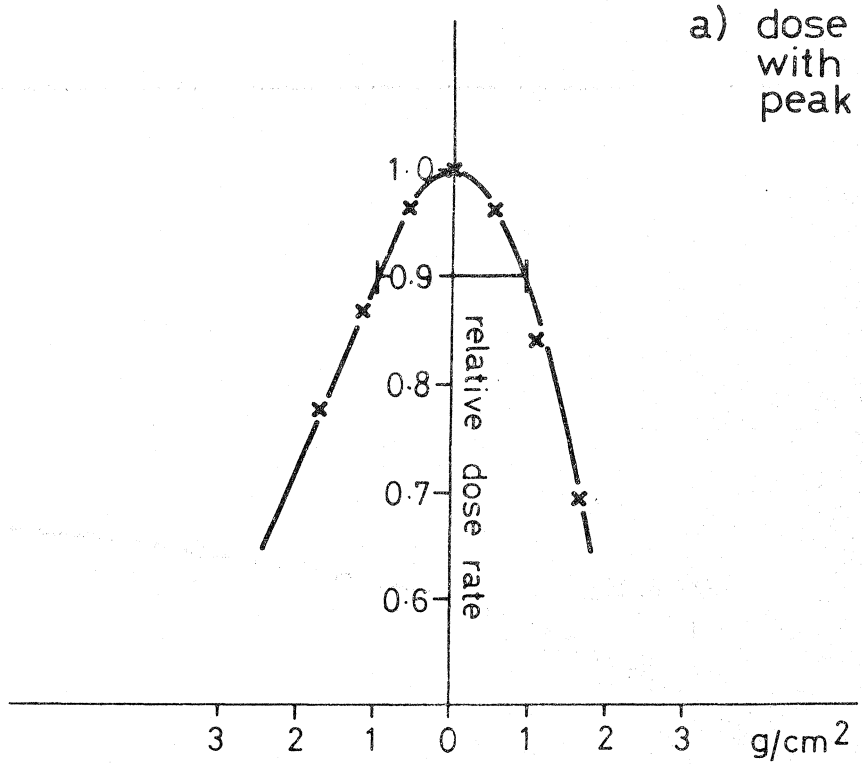

b) dose rate contours across beam at peak

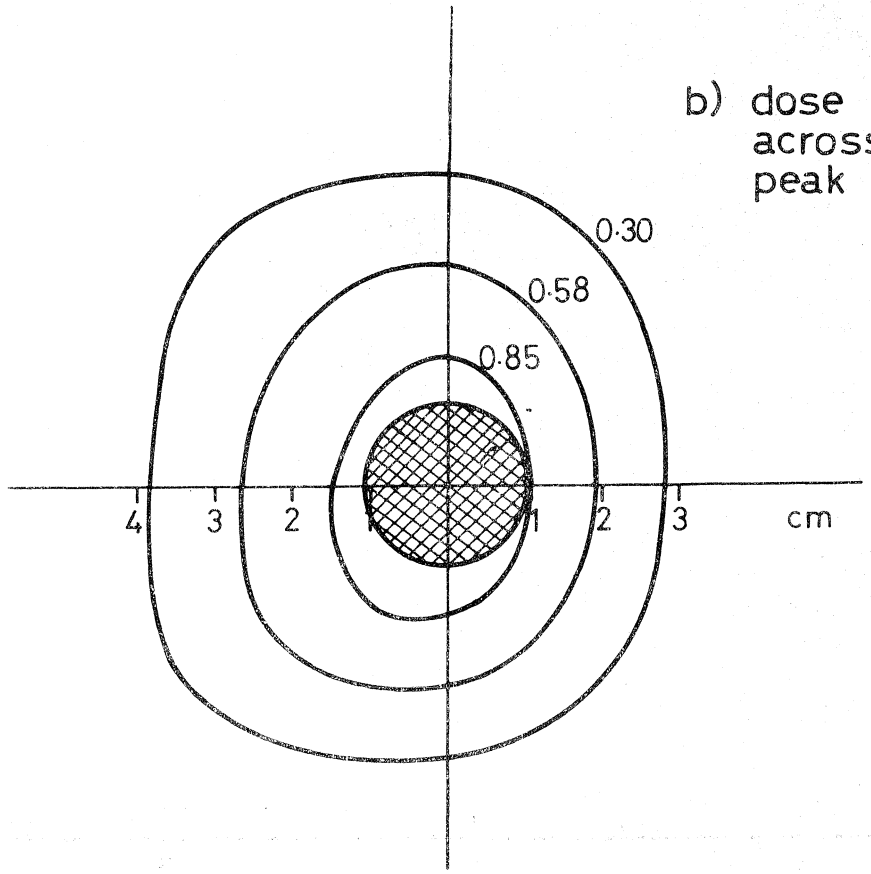

Fig. 3

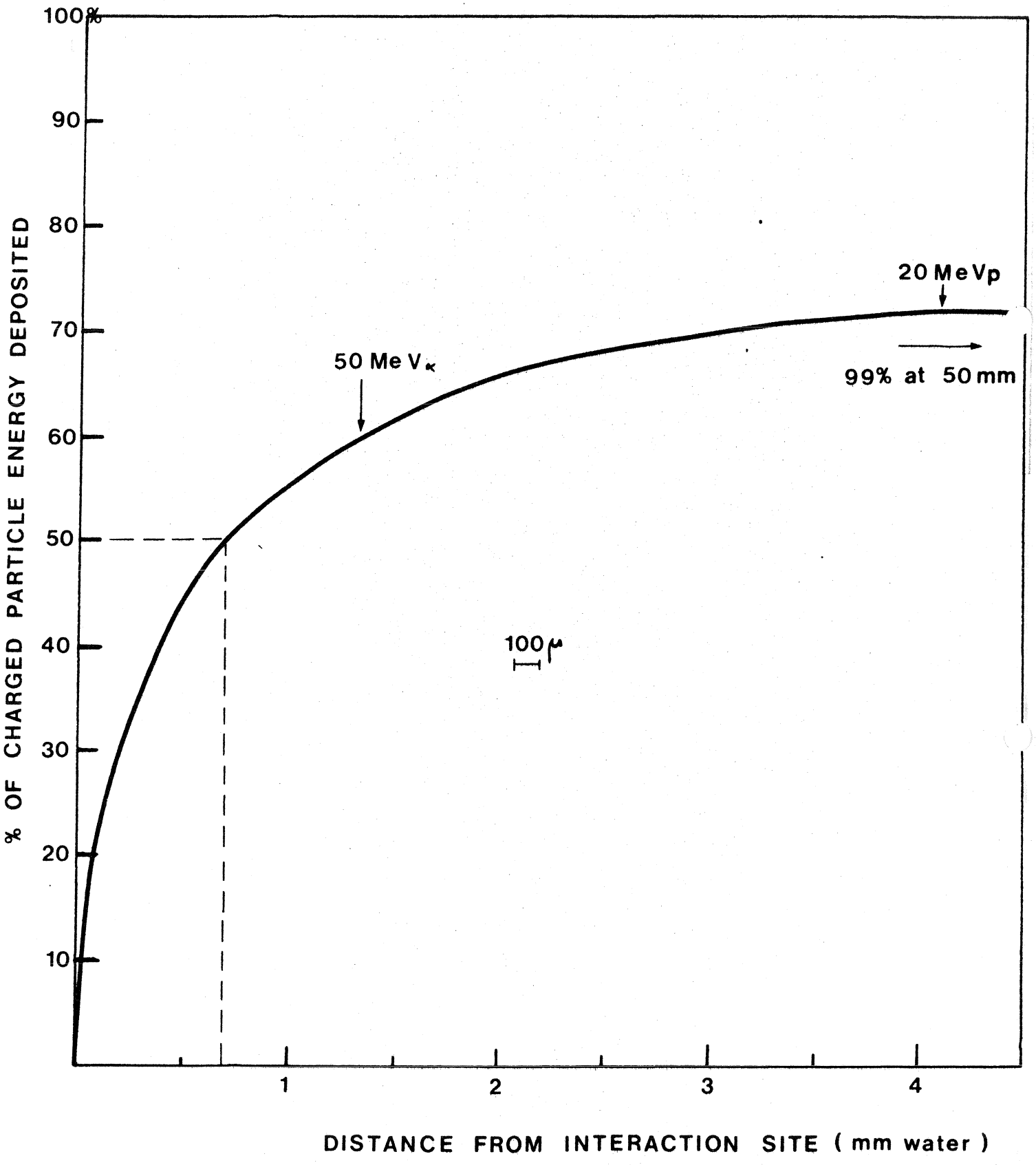
100%
90
80
70
60
50
40
30
20
10
% OF CHARGED PARTICLE ENERGY DEPOSITED
20 MeVp
50 MeV∝
99% at 50 mm
100μ
1
2
3
4
DISTANCE FROM INTERACTION SITE (mm water)

FIG.4

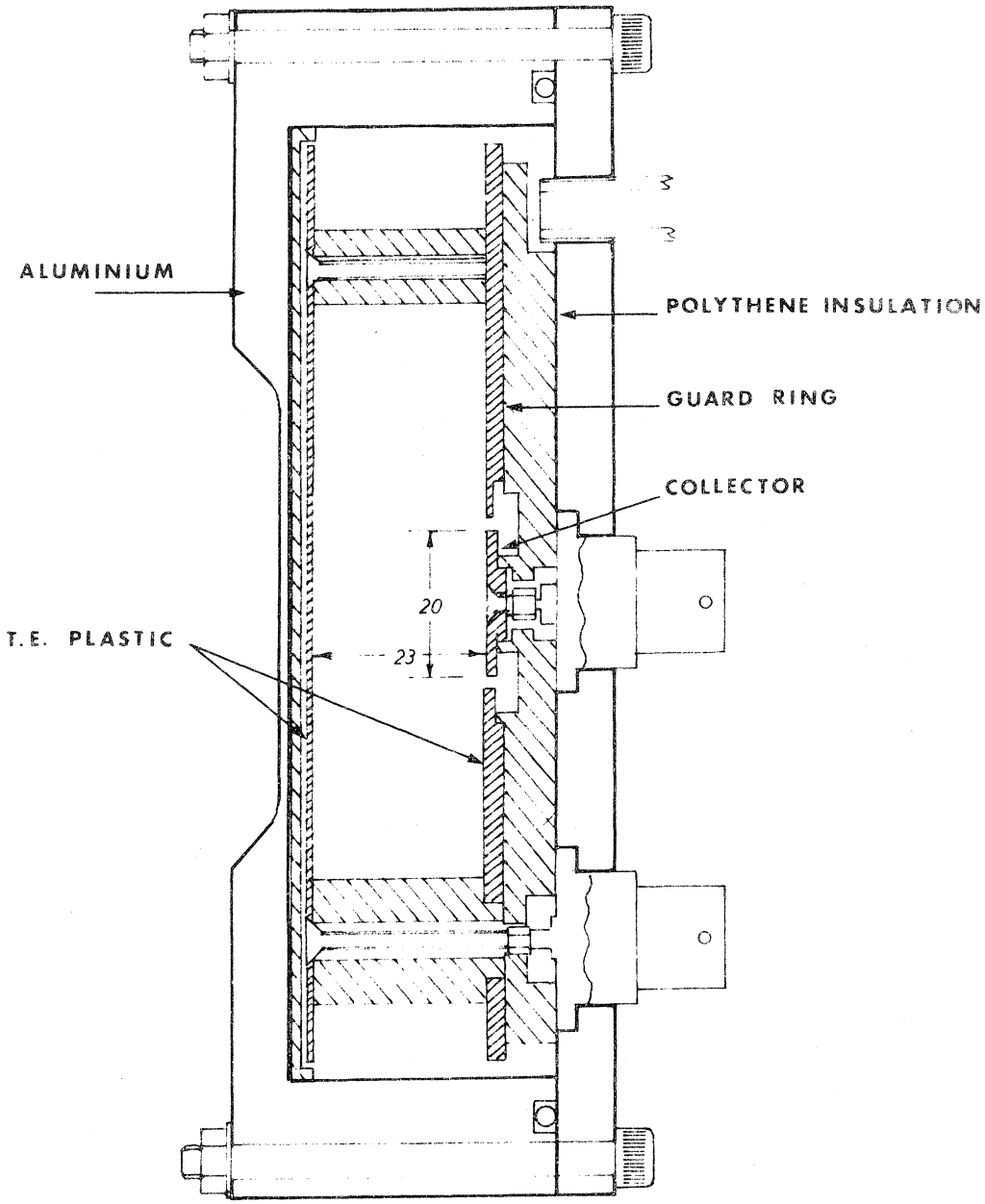

DESIGN OF A BEAM DOSEMETER

FIG. 5